Mathematical modeling and performance analysis of an integrated solar heating and cooling system driven by parabolic trough collector and double-effect absorption chiller

Xuejing Zheng [1, 2], Rui Shi [1], Yaran Wang [1, 2, *], Shijun You [1, 2], Huan Zhang [1, 2], Junbao Xia [3], Shen Wei [4]

[1] School of Environmental Science and Engineering, Tianjin University, Tianjin 300350, China.

[2] Key Laboratory of Efficient Utilization of Low and Medium Grade Energy (Tianjin University), Ministry of Education of China, Tianjin 300350, China.

[3] Science and Technology on Reactor System Design Technology Laboratory, Nuclear Power Institute of China, Chengdu 610213, Sichuan, China.

[4] The Bartlett School of Construction and Project Management, University College London (UCL), 1-19 Torrington Place, London WC1E 7HB, United Kingdom.

[*]Corresponding author: Tel./Fax: +86 2227400832. E-mail addresses: yaran_wang@tju.edu.cn.

Abstract:

With the increasing concerns on energy conservation and environmental protection, solar heating and cooling (SHC) system represents an attractive candidate in building sector. In this paper, an integrated SHC system driven by parabolic trough collector (PTC) and double-effect H_2O/LiBr absorption chiller was presented. The energy generated by solar collectors was supplied to the absorption chiller during the cooling period, and was directly used for space heating with the integration of plate heat exchanger during the heating period. The mathematical models of the whole system including the collector, the double-effect absorption chiller and the plate heat exchanger were established and were validated by field tests. Based on the proposed models, comparison of the SHC system and the conventional gas-driven absorption heating and cooling system was carried out by case study. The annual performances as well as energetic, economic and environmental assessments of the proposed system were investigated. Results show that, 21.3% of the primary energy consumption and 18.8% of the CO_2 emission can be reduced in SHC system. Therefore, the proposed integrated solar heating and cooling system has a promising application prospect in sustainable development in view of its considerable energy saving benefits, potential economic viability and environmental friendly characteristics.

Keywords:

Solar Heating and Cooling; Double-effect Absorption Refrigeration; Parabolic Trough Collector; Energetic, Economic and Environmental (3E) assessment

Nomenclature

a	solution circulation ratio [kg/kg]
A	annual operating cost [RMB]
b	constant matrix
c_p	specific heat [J/kg·K]
C	initial cost [RMB]
CDE	carbon dioxide emission [ton]
COP	coefficient of performance
d	diameter [m]
D	refrigerant mass flow rate [kg/s]
E	annual energy consumption [kWh]
EF	CO_2 emission factor
f	focal distance [m]
F	area [m^2]
G	flow rate (kg/s)
h	convective heat transfer coefficient [$W/m^2 \cdot K$]
H	enthalpy [J]
I	direct normal irradiance [W/m^2]
K	heat transfer coefficient [$W/m^2 \cdot K$]
l	length [m]
M	coefficient matrix
PBP	static payback period [year]
PEC	primary energy consumption [MWh]
PEF	primary energy factor
PER	primary energy ratio
PES	primary energy saving [MWh]
Q	heat transfer [W]
R	fouling resistance [$m^2 \cdot K/W$]
S	solar irradiation absorption [W]
ΔT	temperature difference [K]
T	temperature [K]
u	velocity [m/s]
W	width [m]
x	concentration of the solution [%]
y	steam production ratio [kg/kg]
Greek symbols	
η	intercept factor

η_{IAM}	incidence angle modifier
η_{end}	geometrical end loss
α	absorptivity
ρ	reflectivity
ε	emissivity
τ	transmittance
σ	Stefan-Boltzmann constant [$W/m^2 \cdot K^4$]
θ	incidence angle [°]
λ	heat conductivity coefficient [W/m·K]
υ	density [kg/m^3]
ψ_b	burner combustion ratio [%]
ξ	efficiency
δ	thickness [m]
Subscripts	
a	ambient environment
A	absorber
c	collector
cap	heating/cooling capacity
ch	chilled water
conv	convection
cw	cooling water
ex	external
E	electricity
f	heat transfer fluid
g	glass envelope
h	strong solution
hex	high temperature heat exchanger
hpg	high pressure generator
hw	hot water
in	internal
int	inlet
k	condenser
l	weak solution
lex	low temperature heat exchanger
LiBr	lithium bromide solution
lpg	low pressure generator

m	medium strong solution
NG	natural gas
out	outlet
r	receiver tube
rad	radiation
re	refrigerant
ref	reference
sky	sky
0	evaporator
1, 2,…, 15	state point
Abbreviations	
ABS	absorber
CON	condenser
EVA	evaporator
3E	energetic, economic and environmental
GHC	gas-driven absorption heating and cooling
HEX	high temperature heat exchanger
HPG	high pressure generator
LEX	low temperature heat exchanger
LPG	low pressure generator
PHE	plate heat exchanger
PTC	parabolic trough collector
SHC	solar heating and cooling

1. Introduction

The use of conventional air conditioning system based on vapor compression chillers dominates nearly 50% of the primary energy consumption and accounts for about 40% of greenhouse gas emission in building sectors [1,2]. Research on energy saving and environment benign alternatives for air conditioning has become a global priority [3]. Of the many potential renewable solutions, solar heating and cooling (SHC) system represents an attractive candidate for the merits of energy efficiency enhancement and negligible environmental impact [4].

In SHC systems, the thermal energy generated by solar collectors may be directly used for space heating, producing domestic hot water or supplied to absorption chillers for cooling [5,6]. To ensure continuous and stable operation of the system, thermal energy storage system or back-up energy source is usually considered [7].

For direct heating utilization, solar water heating system is widely accepted with the advantages of mature technology based and low life cycle cost [8]. Depending on whether the hot water is heated in the solar collectors or in a heat exchanger, direct system and indirect system can be defined. Benefiting from the separation of the solar collector loop and hot water loop, the indirect system can operate when the ambient temperature is under 0°C [9].

For cooling energy production, the integration of solar thermal collector with absorption chiller has attained a significant attention, due to its reliability and high efficiency [10,11]. The most common working fluid pairs are water-lithium bromide

(H_2O-LiBr) for temperature levels greater than 4℃ such as for air-conditioning applications, and ammonia-water (NH_3-H_2O) for producing cooling in extremely low-temperature levels such as for refrigeration purpose and industrial application [12,13]. The types of absorption chillers are classified on the basis of their thermodynamic cycle of operation [14]. The advantages of moving toward a higher effect cycle are to enhance the coefficient of performance (COP) of the chiller and to potentially save collector area, if a high temperature heat source is available [15]. The COP of the single-effect chillers is limited to around 0.7 with the driving heat source temperature around 80~100℃. Benefiting from two cascading generators, the COP of double-effect absorption chiller can reach up to 1.42, while the required driving temperature is around 150~200℃ [16]. The types of the employed solar thermal collectors critically depend on the number of effects. Among the various types of thermal collectors driving double-effect absorption chillers, parabolic trough collector (PTC) has a considerable solar fraction and a satisfactory thermal efficiency due to high concentration ratio (around 15~50) and low heat loss levels [17]. The optimistic application potential of PTC to feed double-effect absorption chillers has been pointed out and summarized by Cabrera et al.[18].

The solar-assisted single-effect absorption refrigeration has been extensively studied [19,20]. Numerous experimental analysis and simulation studies have been conducted with regard to parametric optimization [21], performance improvement [22], thermal energy storage [23], auxiliary energy alternative [24], energetic [25] and economic analysis [26] etc. The alternative designs [27], thermal enhancement methods

[28], daily performance [29] and working fluid investigation [30] of PTC also have been carried out among the available literatures. While the simulation and modeling as well as the performance analysis of the double-effect absorption system driven by PTC require more research [31]. The superiorities of double-effect absorption chiller over single-effect absorption chiller [32,33] and PTC over other thermal collectors [34] have been demonstrated, respectively. The energy saving capability of integrating PTC with double-effect absorption chiller has also been pointed out based on computer-code model compared with several SHC systems for different climates [35]. A parametric optimization of a small-scale SHC absorption prototype is presented [36] and the results show that a properly designed system can potentially supply 39% of the cooling and 20% of the heating demand of the building. In general, many of the studies and research papers focus on the performances of PTC-powered double-effect absorption system for space cooling. The studies prove that 50% of the cooling load could be covered [37], 69.47% of the solar energy utilization efficiency could be achieved [38] and 65% of the annual operating costs could be reduced [39]. The contribution to CO_2 emission reduction of solar-assisted double-effect chillers is also pointed out compared to conventional cooling system [40]. The comparison of different working pairs for double-effect absorption chiller powered by PTC is investigated to enhance the advantages of solar cooling system [41]. Analogously, despite some operating behaviors of the SHC systems are taken into account [42], many of which have not considered the annual operation by supplying both cooling and heating demand of

buildings by solar thermal energy [31]. And to supplement this part of the research could exploit the advantage of solar energy from annual dimension. Due to the varying compatibility between solar source supply and load demand during heating and cooling period, reasonable system form and operation mode therefore need to be considered. The corresponding modeling simulation methods for annual system performance analysis also need to be determined and improved.

To access the performance prediction of the SHC system over long periods of time, simulation method based on equation solver is quite extensively used [43]. Therefore, mathematical models are required. Some mathematical modeling of the PTC [44,45] and absorption chiller [46] are developed respectively for applicability illustration. Nevertheless, considering the performance interactions of the PTC and the absorption chiller in practical, the annual system performance assessment and energy consumption analysis need overall consideration. Therefore, integrated heat transfer models of the whole system need to be considered for accurate prediction of the system performance. Then, on the basis of the models, simulations for energetic, economic and environmental performances of the SHC system can be carried out.

This paper presented a solar-assisted heating and cooling system which consisted of PTC, double-effect H_2O/LiBr absorption chiller and plate heat exchanger (PHE). Firstly, the SHC system was described in detail. The operational modes during the cooling period and heating period were proposed. The working process of the absorption chiller and the heat transfer mechanism of the PTC were analyzed. Secondly, the heat transfer models of the whole system including the PTC, the double-effect absorption chiller and the PHE were established in order to analyze the performance of the system. The proposed SHC system was designed and applied on an office building in Tianjin (China). Several field tests were carried out and the models were validated. Thirdly, the energetic, economic and environmental (3E) assessment method were introduced respectively. A building model in the prototype of the office building was developed. Finally, the simulation study was illustrated on the basis of the proposed mathematical models. The annual performances as well as energetic, economic and environmental (3E) assessments of the proposed SHC system were investigated compared with conventional gas-driven absorption heating and cooling (GHC) system. The energy saving potential, economic viability and CO_2 emission reduction effect were demonstrated.

2. System description

The major apparatuses of the SHC system are PTC, double-effect H_2O/LiBr absorption chiller and PHE. The SHC system can be divided into solar collector loop and load loop. The solar collector loop mainly consists of PTC which generates and supplies thermal energy to the absorption chiller for cooling or provides heating via PHE. The load loop comprises the double-effect absorption chiller loop and the PHE loop, which cover the building loads with the circuits of chilled water and hot water through the evaporator and the PHE respectively. The gas burner equipped in high pressure generator is used as a backup heater in case of solar energy shortage. The schematic diagram of the SHC system is illustrated in Fig. 1.

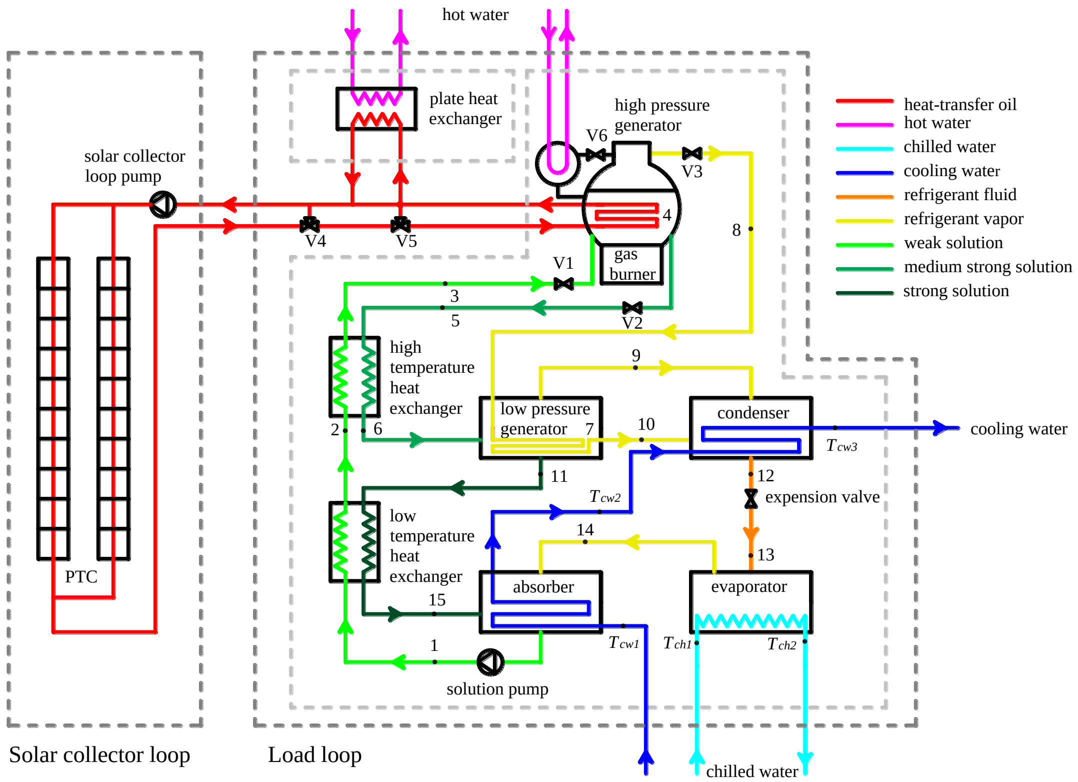

Fig. 1 Schematic diagram of the SHC system

During the cooling period, valve V1, valve V2, valve V3 are opened and valve V6 is closed. The heat-transfer oil in PTC can be heated to 100℃~250℃. With the high pressure generator branch opened by three-way valve V5, the thermal energy generated by PTC can be supplied to the absorption chiller, thus refrigerant vapor could be boiled off from weak solution. During the early period of system operation, the heat-transfer oil is circulated in the collectors and heated by solar radiation with valve V4 closed. The high pressure generator branch will be opened after the temperature of heat-transfer oil meet the absorption chiller driven requirement. Under the priority of using solar power, the double-effect refrigeration system can be powered by solar thermal and gas fired independently or simultaneously, depending on the intensity of the solar radiation.

During the heating period, valve V1, valve V2, valve V3 are closed. The heat-transfer oil in PTC is heated to low temperature (＜100℃). The thermal energy derived by PTC is directly used for heating purpose coupled with PHE. With the branch of PHE opened by three-way valve V5, hot water can be supplied. Analogously, if the harvested solar energy is not adequate for building demand, the gas burner installed in generator will be activated. The heat-transfer oil is preheated in the collectors in the same way as cooling condition.

2.1 The PTC

The PTC consists of parabolic trough shaped reflector, surface treated metallic receiver tube, evacuated glass envelope, support structure and tracking mechanism. The reflector concentrates direct solar radiation onto the receiver located at its focal line and heats the transfer fluid in the tube. Fig. 2 illustrates the heat transfer model in a cross section of the PTC.

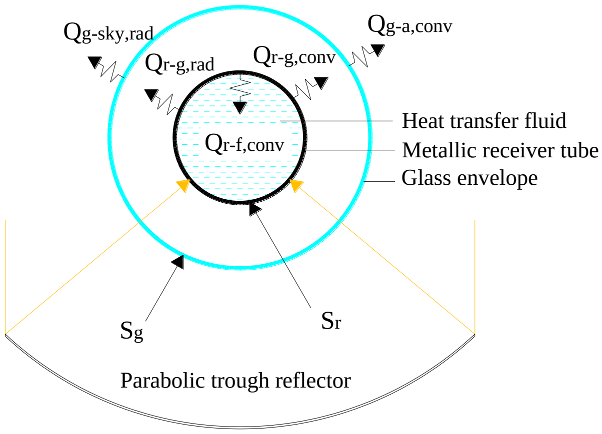

Fig. 2 Heat transfer model in a cross section of the PTC

The detailed heat transfer process of the PTC is as follows: the incident solar radiation is reflected by the parabolic trough shaped mirrors and concentrated at heat collector element. A small amount of the radiation is absorbed by the glass envelope S_g and the remaining is transmitted and absorbed by the receiver tube S_r. A part of the absorption energy is transferred to the heat transfer fluid by forced convection $Q_{r\text{-}f,conv}$ and the other part is returned to the glass envelope by natural convention $Q_{r\text{-}g,conv}$ and radiation $Q_{r\text{-}g,rad}$. The energy coming from the receiver tube (convention and radiation) pass through the glass envelope and along with the absorbed energy by the glass envelope, is lost to the environment by convention $Q_{g\text{-}a,conv}$ and to the sky by radiation $Q_{g\text{-}sky,rad}$.

2.2 The absorption chiller

The double-effect absorption chiller consists of seven main heat exchangers: evaporator (EVA), absorber (ABS), condenser (CON), low pressure generator (LPG), high pressure generator (HPG), low temperature heat exchanger (LEX) and high temperature heat exchanger (HEX).

The working process of the chiller is as follows: the weak solution (state 1) pumps through the LEX (state 2) and HEX (state 3) successively, and then is heated in the HPG (state 4), turning into the medium strong solution (state 5) and refrigerant vapor (state 8). The thermal energy is provided by either the PTC or the natural gas burner. The medium strong solution passes through the HEX (state 6), gets heated in the LPG (state 7) by the refrigerant vapor extracted from the HPG, and turns into strong solution (state

11) and refrigerant vapor (state 9). The strong solution goes through the LEX (state 15) and flows into the ABS. The generated refrigerant vapor (state 9 and state 10) enters into the CON together and is cooled into liquid (state 12). The liquid refrigerant via the expansion valve (state 13) goes into the EVA, becomes low pressure vapor (state 14), enters into the ABS and is absorbed by the strong solution. The main state points from 1 to 15 are represented in Fig. 1.

3. Model development

The integrated heat transfer models of the whole system including the PTC, the double-effect absorption chiller and the PHE are established in Section 3.1 to Section 3.3. And the validations of the models are presented in Section 3.4.

3.1 PTC model

The mathematical model of the PTC consists of the energy conservation equations of glass envelope, metallic receiver tube and heat transfer fluid. For simplicity, the following assumptions are made [47,48]:

- The heat transfer process is steady.
- The heat flux around the circumference of the receiver tube and glass envelope is uniform.
- The glass envelope is opaque to infrared radiation.
- Only direct solar radiation is considered.
- Heat loss through the supports is neglected.
- Multiple reflections between receiver tube and glass envelope are neglected.

(1) Glass envelope

The energy conservation equation of the glass envelope is expressed as follows:

$$S_{\mathrm{g}} + Q_{\text{r-g,conv}} + Q_{\text{r-g,rad}} - Q_{\text{g-a,conv}} - Q_{\text{g-sky,rad}} = 0 \tag{1}$$

In Eq. (1), the total solar irradiation absorption of the glass envelope S_{g} can be calculated by:

$$S_{\mathrm{g}} = \eta_1\eta_2\eta_3\eta_4\eta_5\eta_6\rho_c \cdot \eta_{IAM} \cdot \eta_{end} \cdot \alpha_{\mathrm{g}} \cdot W_{\mathrm{c}} \cdot l_{\mathrm{c}} \cdot I \tag{2}$$

where $\eta_1 \sim \eta_6$ are intercept factors accounted for the macroscopic imperfections [49,50]; η_{IAM} is incidence angle modifier which quantifies the optical losses [49,51]; η_{end} is the geometrical end losses caused by the off-normal incidence angle [52]. The incidence angle (θ) is a function of tracking mode and orientation of the PTC [53].

The convection heat transfer between glass envelope and receiver tube $Q_{\text{r-g,conv}}$ is determined by:

$$Q_{\text{r-g,conv}} = \pi d_{\text{r,ex}} l_{\mathrm{c}} h_{\text{r-g}} \left(T_{\mathrm{r}} - T_{\mathrm{g}}\right) \tag{3}$$

in which the convective heat transfer coefficient $h_{\text{r-g}}$ is referred from Ref. [44], considering the vacuum treatment.

The radiation heat transfer between glass envelope and receiver tube $Q_{\text{r-g,rad}}$ can be obtained by:

$$Q_{\text{r-g,rad}} = \frac{\sigma\left(T_{\mathrm{r}}^4 - T_{\mathrm{g}}^4\right)}{\left(1-\varepsilon_{\mathrm{g}}\right)/\left(\pi d_{\text{g,in}} l_{\mathrm{c}} \varepsilon_{\mathrm{g}}\right) + 1/\left(\pi d_{\text{r,ex}} l_{\mathrm{c}}\right) + \left(1-\varepsilon_{\mathrm{r}}\right)/\left(\pi d_{\text{r,ex}} l_{\mathrm{c}} \varepsilon_{\mathrm{r}}\right)} \tag{4}$$

The convection heat transfer between glass tube and ambient air $Q_{\text{g-a,conv}}$ is given as:

$$Q_{\text{g-a,conv}} = \pi d_{\text{g,ex}} l_{\text{c}} h_{\text{g-a}} \left(T_{\text{g}} - T_{\text{a}}\right) \tag{5}$$

where the calculation of the $h_{\text{g-a}}$ depends on the regime of convective heat transfer and is referred from Ref. [54,55].

The radiation heat transfer between glass envelope and sky $Q_{\text{g-sky,rad}}$ can be calculated as:

$$Q_{\text{g-s,rad}} = \sigma \pi d_{\text{g,ex}} l_{\text{c}} \varepsilon_{\text{g}} \left(T_{\text{g}}^{4} - T_{\text{sky}}{}^{4}\right) \tag{6}$$

where the sky temperature T_{sky} (K) is given as:

$$T_{\text{sky}} = 0.0552 T_{\text{a}}^{1.5} \tag{7}$$

(2) Receiver tube

The energy conservation equation of the receiver tube is expressed as follows:

$$S_{\text{r}} - Q_{\text{r-g,conv}} - Q_{\text{r-f,conv}} - Q_{\text{r-g,rad}} = 0 \tag{8}$$

The total solar irradiation absorption of the receiver tube S_{r} can be calculated as:

$$S_{\text{r}} = \eta_1 \eta_2 \eta_3 \eta_4 \eta_5 \eta_6 \rho_c \cdot \eta_{IAM} \cdot \eta_{end} \cdot \tau_{\text{g}} \cdot \alpha_{\text{r}} \cdot W_{\text{c}} \cdot l_{\text{c}} \cdot I \tag{9}$$

The convection heat transfer between receiver tube and heat transfer fluid $Q_{\text{r-f,conv}}$ can be obtained by:

$$Q_{\text{r-f,conv}} = \pi d_{\text{r,in}} l_{\text{c}} h_{\text{r-f}} \left(T_{\text{r}} - T_{\text{f}}\right) \tag{10}$$

in which the $h_{\text{r-g}}$ can be calculated with Ref. [56,57], considering the transitional or turbulent condition of the heat transfer fluid.

(3) Heat transfer fluid

The energy conservation equation of heat transfer fluid is expressed as follows:

$$\upsilon_{\mathrm{f}} c_{p,\mathrm{f}} u_{\mathrm{f}} \pi \frac{d_{\mathrm{r,in}}^{2}}{4} (T_{\mathrm{f,int}} - T_{\mathrm{f,out}}) + Q_{\mathrm{r\text{-}f,conv}} = 0 \tag{11}$$

(4)Efficiency

The collector efficiency of the PTC can be calculated by [47]:

$$\xi_{\mathrm{c}} = \frac{Q_{\mathrm{c}}}{W_{\mathrm{c}} \cdot l_{\mathrm{c}} \cdot I} = \frac{\upsilon_{\mathrm{f}} c_{p,\mathrm{f}} u_{\mathrm{f}} \pi d_{\mathrm{r,in}}^{2} (T_{\mathrm{f,int}} - T_{\mathrm{f,out}})}{4 W_{\mathrm{c}} \cdot l_{\mathrm{c}} \cdot I} \tag{12}$$

3.2 Double-effect absorption chiller model

The mathematical model of the absorption chiller consists of mass conservation equations, energy conservation equations and heat transfer equations of the seven main heat exchangers (EVA, ABS, CON, LPG, HPG, LEX and HEX). The correlations between the working medium flow rates are also given in this section. Before describing the mathematical equations, the main assumptions are taken into account as follows [34,46,58]:

- The heat and mass transfer process is under steady state.
- The pressure of CON and LPG are identical.
- The solutions leaving ABS, HPG, and LPG are saturated.
- The refrigerants leaving the CON and the EVA are saturated.
- Heat loss to the environment is neglected.
- The pressure drops of the pipes and vessels are neglected and the solution pump energy is neglected.

(1) Mass conservation equations

Based on the mass balance of each component, the mass conservation equations are expressed as follows:

$$a x_{\mathrm{l}} = (a-1) x_{\mathrm{h}} \tag{13}$$

$$a x_{\mathrm{l}} = (a-y) x_{\mathrm{m}} \tag{14}$$

(2) Energy conservation equations

Based on the energy balance of each component, the energy conservation equations are as follows:

$$Q_{i,1} = -Q_{i,2} \tag{15}$$

$$Q_{i,1} = (GH)_{i,\mathrm{LiBr,int}} + (DH)_{i,\mathrm{re,int}} - (GH)_{i,\mathrm{LiBr,out}} - (DH)_{i,\mathrm{re,out}} \tag{16}$$

$$Q_{i,2} = c_{p,i} G_i (T_{i,\mathrm{int}} - T_{i,\mathrm{out}}) \tag{17}$$

where i could be 0, A, k, lpg.

For the HPG, $Q_{\mathrm{hpg},1}$ is calculated with Eq. (16) (i=hpg), while $Q_{\mathrm{hpg},2}$ is obtained by Eq. (18).

$$Q_{\mathrm{hpg},2} = c_{p,\mathrm{f}} G_{\mathrm{f}} (T_{\mathrm{f,int}} - T_{\mathrm{f,out}}) + \psi_b Q_{\mathrm{NG}} \tag{18}$$

where ψ_b is burner combustion ratio (%).

For the LEX and HEX, the energy conservation equations are:

$$Q_{i,1} = -Q_{i,2} \tag{19}$$

$$Q_{i,1} = (GH)_{i,\mathrm{l,int}} - (GH)_{i,\mathrm{l,out}} \tag{20}$$

$$Q_{i,2} = (GH)_{i,j,\mathrm{int}} - (GH)_{i,j,\mathrm{out}} \tag{21}$$

while i=lex, j=h; i=hex, j=m.

(3) Heat transfer equations

The heat transfer equation is described as follows:

$$Q_{i,3} = K_i F_i \frac{\Delta T_{i,2} - \Delta T_{i,1}}{\ln \frac{\Delta T_{i,2}}{\Delta T_{i,1}}} \tag{22}$$

where $\Delta T_{i,1}$ stands for the smaller temperature difference of the two heat exchange fluid in component *i*, $\Delta T_{i,2}$ stands for the larger one.

The total heat transfer coefficient K_i of the component *i* can be calculated as:

$$\frac{1}{K_i} = \frac{1}{h_{i,\mathrm{ex}}} + \frac{1}{h_{i,\mathrm{in}}}\left(\frac{d_{i,\mathrm{ex}}}{d_{i,\mathrm{in}}}\right) + \frac{d_{i,\mathrm{ex}}}{2\lambda_i} \ln \frac{d_{i,\mathrm{ex}}}{d_{i,\mathrm{in}}} \tag{23}$$

in which *i* could be 0, A, k, lex, hex, lpg, hpg. The calculations of the convective heat transfer coefficients are referred from the Ref. [59].

(4) Flow rate of working medium

The flow rate of the working medium can be calculated as follows:

$$G_1 = aD \tag{24}$$

$$G_\mathrm{A} = (a-1)D \tag{25}$$

The refrigerant flow rate in the HPG and LPG can be calculated by Eqs. (26) and (27).

$$G_{\mathrm{hpg,re}} = yD \tag{26}$$

$$G_{\mathrm{lpg,re}} = (1-y)D \tag{27}$$

(5) Energy consumption index

The COP of the double-effect absorption chiller is defined as:

$$COP = \frac{Q_0}{Q_{\mathrm{hpg}}} \tag{28}$$

3.3 PHE model

For the PHE models, the energy conservation equations and the heat transfer equation are employed. And some assumptions are made as follows [60]:

- Heat loss to the surroundings is neglected.
- PHE operates under steady-state conditions.
- All the physical properties are constants.
- Phase of each fluid does not change in the flowing process.
- No heat exchange in the direction of flow.
- Distribution of flow through the channels of a pass is uniform.

The energy conservation equations are given by:

$$Q_{\mathrm{PHE},1} = -Q_{\mathrm{PHE},2} \tag{29}$$

$$Q_{\mathrm{PHE},1} = c_{p,\mathrm{f}} G_{\mathrm{f}} (T_{\mathrm{f,PHE,int}} - T_{\mathrm{f,PHE,out}}) + \psi_b Q_{\mathrm{NG}} \tag{30}$$

$$Q_{\mathrm{PHE},2} = c_{p,\mathrm{hw}} G_{\mathrm{hw}} (T_{\mathrm{hw,int}} - T_{\mathrm{hw,out}}) \tag{31}$$

where the values of the $T_{\mathrm{f,PHE,int}}$ and $T_{\mathrm{f,PHE,out}}$ in PHE are equal to the values of $T_{\mathrm{f,out}}$ and $T_{\mathrm{f,int}}$ in PTC, respectively.

The heat transfer equation is the same as Eq. (22) (i=PHE), in which the total heat transfer coefficient K can be obtained by:

$$\frac{1}{K_{\mathrm{PHE}}} = \frac{1}{K_{\mathrm{f}}} + R_{\mathrm{f}} + \frac{\delta_{\mathrm{PHE}}}{\lambda_{\mathrm{PHE}}} + R_{\mathrm{hw}} + \frac{1}{K_{\mathrm{hw}}} \tag{32}$$

where R_{f} and R_{hw} represent the fouling resistances on the plate surfaces corresponding to the heat-transfer oil side and the hot water side, respectively.

Due to the complexity and mutual restraint between the temperature and concentration range of the solution, the models are solved using the subspace trust region method based on Newton [61] in the optimization toolbox of scientific computing software. The simulation flow chart of the proposed mathematical models is shown in Fig. 3.

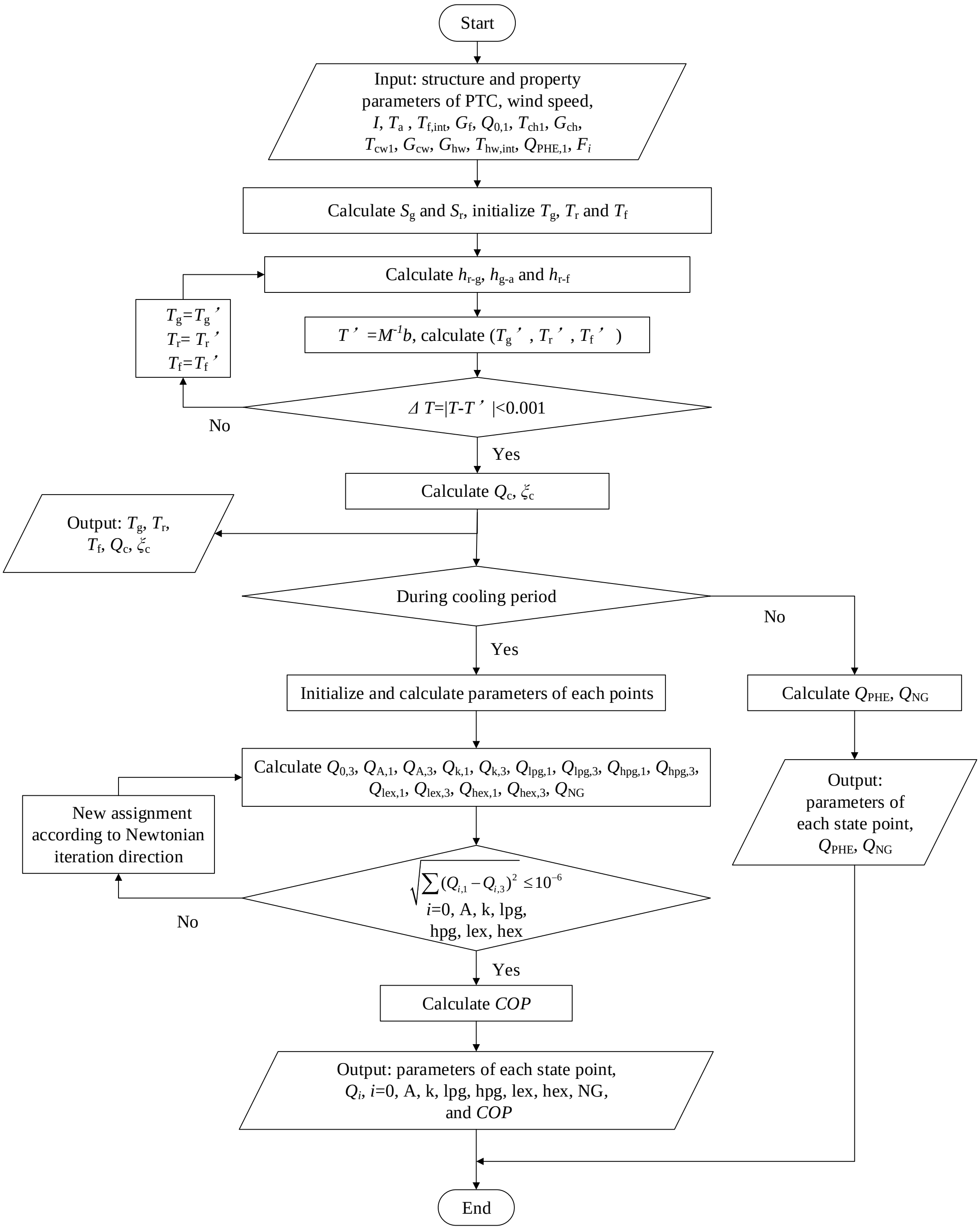

Fig. 3 Simulation flow chart of the proposed mathematical models

3.4 Model validation

In order to verify the accuracy and reliability of the proposed heat transfer models, a PTC operated double-effect H_2O/LiBr absorption SHC system was designed and applied on an office building in Tianjin (China). Several field tests were carried out. The installed parabolic trough field comprised eight module groups assembled in parallel and fixed on steel support structure in the east-west alignment adopted north-south horizontal axis tracking method. The module groups measured 50m long by 2.5m width each, owing a total of 1000m^2 collecting area. Fig. 4 depicts the photograph of the PTC. Synthetic oil was applied as heat transfer fluid in metallic receiver tubes. The details of the material, optical and geometrical parameters of different components of the PTC are provided in Table 1, and the specific parameters of the absorption chiller are listed in Table 2.

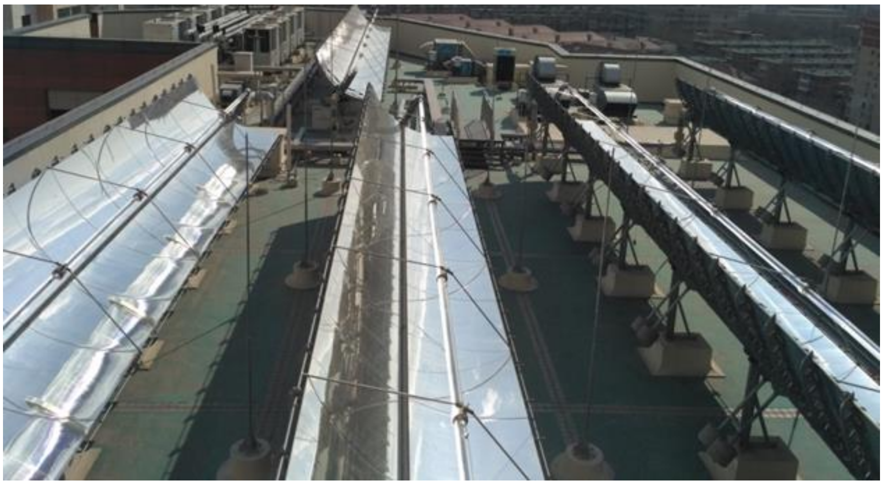

Fig. 4 Photograph of the PTC

Table 1

Parameters of the test PTC

Components	Parameters	Values
Reflector	Material	Low-iron glass

	f_c (m)	0.85
	ρ_c	0.90
Glass envelope	Material	Borosilicate glass
	$d_{g,in}$ / $d_{g,ex}$ (m)	0.096/0.102
	α_g	0.02
	ε_g	0.86
	τ_g	0.90
Metallic receiver	Material	Stainless steel
	$d_{r,in}$ / $d_{r,ex}$ (m)	0.038/0.042
	α_r	0.93
	ε_r	0.11

Table 2
Parameters of the test double-effect H_2O/LiBr absorption chiller

Parameters	Values
Rated refrigerating capacity (kW)	1550
Heat source temperature (K)	433
Heat exchange efficiency (%)	70
$T_{ch,int}$ / $T_{ch,out}$ (K)	286 / 281
$T_{cw,int}$ / $T_{cw,out}$ (K)	303 / 308
F_{hpg} (m^2) / ΔT_{hpg} (K)	66 / 10
F_{lpg} (m^2) / ΔT_{lpg} (K)	96 / 5
F_0 (m^2) / ΔT_0 (K)	225 / 3

F_k (m^2) / ΔT_k (K)	94 / 3
F_{hex} (m^2)	50
F_{lex} (m^2)	26
F_A (m^2)	265

The direct normal solar irradiance was calculated with two solar radiometers (of ±2% W/m^2 accuracy) which measured the total solar irradiance and the scattered solar irradiance, respectively. The solar irradiance was recorded in real time by a data acquisition instrument with a sample interval of 1min. The outdoor air temperature was measured using Temperature-Humidity automatic recorders (of ±0.1 °C and ±1% RH accuracy) with a sample interval of 1min. In order to reduce the test error, average value was taken from three simultaneously recorded instruments. The outdoor wind speed was measured using TSI anemometer (of ±3% m/s accuracy). Other operating parameters were automatically collected and recorded by the system with sampling interval of 1min. Specific information of the instruments are shown in Table 3.

Table 3

Technical parameters of the test devices

Devices	Number	Accuracy	Full Scale	Sampling interval
Solar radiometer	2	±2% W/m^2	0~2000 W/m^2	-
Data acquisition instrument	1	-	-	1min
Temperature-Humidity	3	±0.1 °C	-40~70°C	1min
Automatic recorder		±1% RH	0～100%RH	
TSI anemometer	1	±3% m/s	0~50m/s	1min

In order to verify the accuracy of the PTC model, several heating conditions and cooling conditions were selected. For heating conditions, the direct normal irradiance varied from 500.8 W/m^2~710.2 W/m^2. The outdoor air temperature was in the range of 8.9℃~13.4℃. The outdoor wind speed ranged from 0.7m/s~1.9m/s. For cooling conditions, the direct normal irradiance varied from 650.6 W/m^2~807.4 W/m^2. The outdoor air temperature was in the range of 31.6℃~38.4℃. The outdoor wind speed ranged from 1.2m/s~3.3m/s. Several stable working conditions were also considered in this paper for the double-effect absorption chiller model validation. The inlet temperature of the cooling water varied from 30.3℃~30.5℃. The inlet temperature of the chilled water was in the range of 12.7℃~13.4℃. To verify the models from an overall dimension in system performance, the heat source for the absorption chiller was provided by PTC, and therefore the performance interactions of the PTC and the absorption chiller were considered and reflected. The heat source temperature ranged from 138.2℃~170℃.

Fig.5 (a) and (b) show the comparison between the simulations and test measurements on the outlet temperature of heat-transfer oil during cooling condition and heating condition respectively. The simulated and measured results achieve good agreement. The maximum deviation of heat-transfer oil outlet temperature is 0.55℃ at cooling condition and 0.87℃ at heating condition. Fig.6 shows the simulated and measured results of the PTC efficiency. The simulated efficiency is slightly higher than the measured ones with a difference lower than 5.4%. Considering the heat loss through the bracket and tube ends are ignored in the heat transfer models, the agreement can be considered as reasonably accurate for analyzing and predicting PTC performance.

As it is highlighted in the Fig. 7, the COP in test varies from 1.05 to 1.38. The maximum deviation between simulated results and test measurements is 0.04, accounted for 3.7% error. Fig. 8 shows the variation of COP under different heat source temperature. With the increasing of the heat source temperature, the performance of the absorption chiller improves. This is benefit from the increasing of generation temperature, and the refrigerant evaporation therefore increased. The upward trend becomes relatively slow after the heating source temperature raised above 152.5°C. This can be accounted by the limitation of the heat transfer area in generator. The comparison results indicate that the proposed mathematical models are acceptable for the performance analysis of the SHC system.

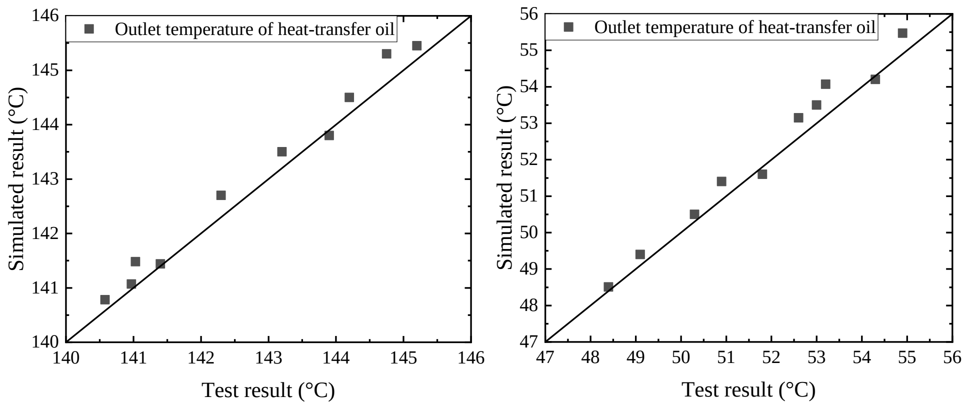

(a) Cooling condition (b) Heating condition

Fig. 5 Comparison results of heat-transfer oil outlet temperature

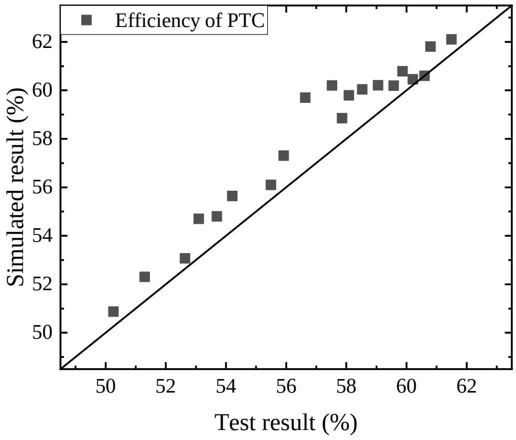

Fig. 6 Comparison results of PTC efficiency

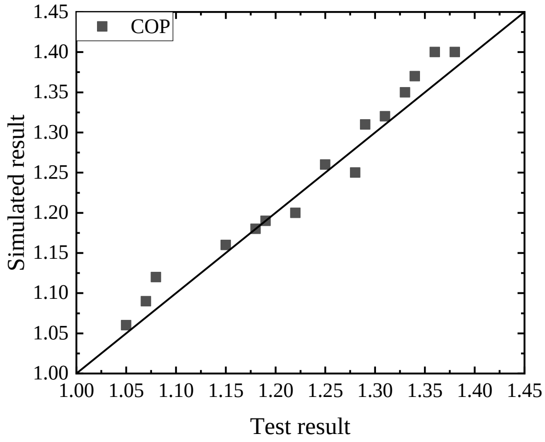

Fig. 7 Comparison results of COP

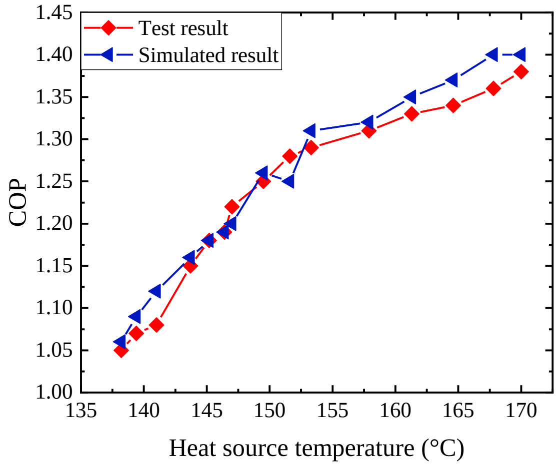

Fig. 8 Variation of COP under different heat source temperature

4. Methodologies of 3E analysis

In this section, the energetic, economic and environmental (3E) assessment methods are introduced respectively. In order to investigate the annual performance of the SHC system, the conventional commonly used gas-driven absorption heating and cooling system (GHC) is selected as the reference.

4.1 Energetic analysis

To estimate the primary energy saving (PES) of the SHC system, the primary energy consumption (PEC) can be calculated by Eqs. (33) and (34), which is commonly expressed to aggregate the non-renewable energy such as natural gas and electricity consumed by each configuration.

$$PEC_{\mathrm{SHC}} = PEF_{\mathrm{E}} \cdot E_{\mathrm{E,SHC}} + PEF_{\mathrm{NG}} \cdot E_{\mathrm{NG,SHC}} \tag{33}$$

$$PEC_{\mathrm{ref}} = PEF_{\mathrm{E}} \cdot E_{\mathrm{E,ref}} + PEF_{\mathrm{NG}} \cdot E_{\mathrm{NG,ref}} \tag{34}$$

where E_{E} and E_{NG} are annual energy consumed of the electric equipment and gas burner respectively; PEF_{E} and PEF_{NG} denote the primary energy factors, which are adopted as 3.58 and 1.64 respectively in this paper [62].

Accordingly, the PES can be obtained as follows:

$$PES = PEC_{\mathrm{ref}} - PEC_{\mathrm{SHC}} \tag{35}$$

In this paper, primary energy ratio (PER) is also calculated by Eqs. (36) and (37) to evaluate the system energy saving potential, which indicates how much usable energy can be generated per primary energy input [63].

$$PER_{\mathrm{SHC}} = \frac{Q_{\mathrm{cap}}}{E_{\mathrm{NG,SHC}} / \xi_{\mathrm{NG}} + E_{\mathrm{E,SHC}} / \xi_{\mathrm{E}}} \tag{36}$$

$$PER_{\mathrm{ref}} = \frac{Q_{\mathrm{cap}}}{E_{\mathrm{NG,ref}} / \xi_{\mathrm{NG}} + E_{\mathrm{E,ref}} / \xi_{\mathrm{E}}} \tag{37}$$

4.2 Economic analysis

The SHC technology is generally characterized by relatively high capital investment and low operational cost. The high initial cost, particularly the cost of the collectors, represents a major economic hurdle for these systems [64]. Therefore, it is necessary to take both capital and operating costs into account in an economic evaluation of the proposed system, in order to enable better long-term decision making.

The payback period (PBP) is adopted as economic criteria in this paper to determine the financial performance on energy efficiency project. The PBP is defined as the length of time required for the cash inflows to recover its initial investment costs. The additional capital investment costs of the SHC system can be compensated over time due to cumulative savings from operating and maintenance costs. Thus the PBP of the SHC system can be estimated from Eq. (38).

$$PBP = \frac{C_{\mathrm{SHC}} - C_{\mathrm{ref}}}{A_{\mathrm{ref}} - A_{\mathrm{SHC}}} \tag{38}$$

where C and A are initial cost and annual operating cost of the system respectively.

4.3 Environmental analysis

Due to the increasing environmental concerns, it is necessary to consider the environmental impacts while designing energy systems [65]. In the present study, the annual carbon dioxide emission (CDE) is estimated to identify the environmental effect, which can be formulated as [15]:

$$CDE = CDE_{\mathrm{E}} + CDE_{\mathrm{NG}} \tag{39}$$

in which

$$CDE_{\mathrm{E}} = E_{\mathrm{E}} \cdot EF_{\mathrm{E}} \tag{40}$$

$$CDE_{\mathrm{NG}} = E_{\mathrm{NG}} \cdot EF_{\mathrm{NG}} \tag{41}$$

where *EF* is CO_2 emission factor.

4.4 Cooling/heating load simulation

In order to conduct the simulations for 3E assessments on the basis of the proposed mathematical models, the aforementioned office building in Section 3.4 is taken as a prototype and the three dimensional design of the building is developed which is shown in Fig. 9.

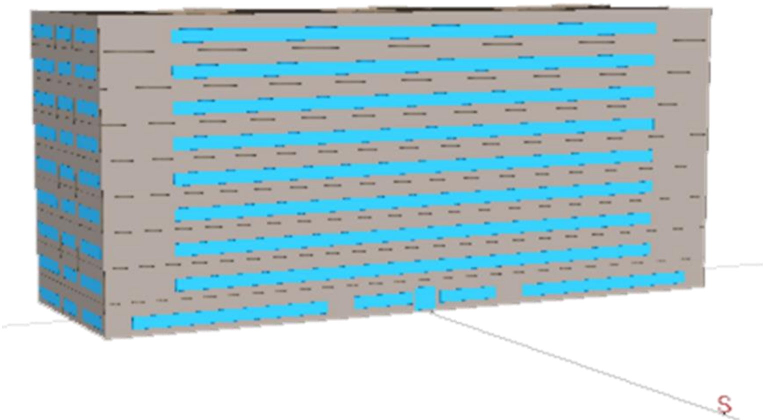

Fig. 9 Three dimensional model of the office building

The office building consists of 9 floors with total air-conditioning area of 18270m^2. The input weather parameters adopt the Chinese Standard Weather Data based on typical meteorological year in energy simulation software [66]. The hourly building loads during cooling period (date 15 Jun to 15 Sep) and heating period (date 15 Nov to next year 15 Mar) are simulated by eQUEST software, which is shown in Fig. 10. The peak cooling load and peak heating load are 1531.7kW and 1258.2kW, respectively.

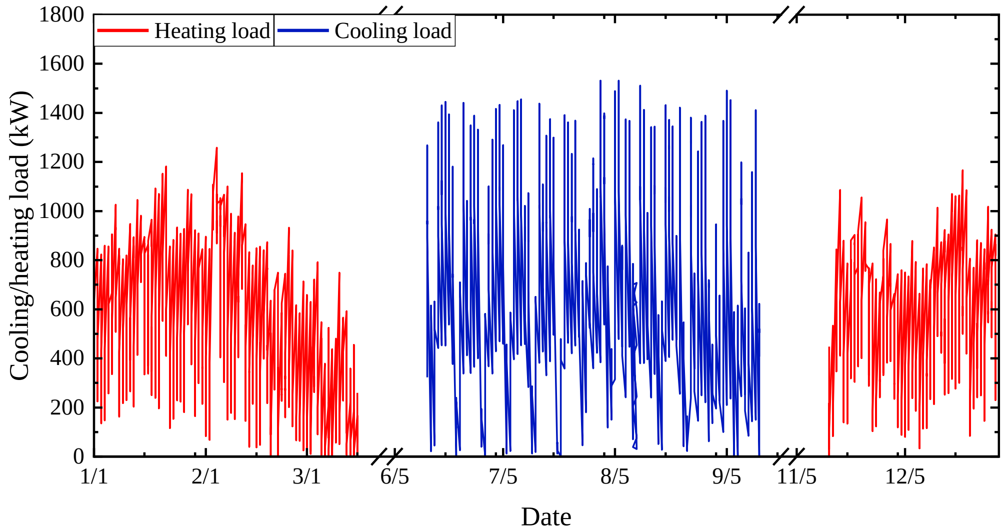

Fig. 10 Cooling/heating loads

5. Results and discussion

5.1 Energetic performance

The hourly solar heat collection of the SHC system is shown in Fig. 11. A basically 500kW of peak solar heat collection during cooling and heating season is depicted, which can be accounted by two reasons. One is the similar efficiency of PTC during heating condition to that during cooling condition, due to the combined effect of efficient operation mode and adverse factors of outdoor environment such as low dry-bulb temperature and high wind speed. The other is the similar peak normal direct solar radiation throughout the year. Besides, the solar heat collection ability during cooling period is more stable than that during heating period, which provides an ideal heat source for the double-effect absorption chiller.

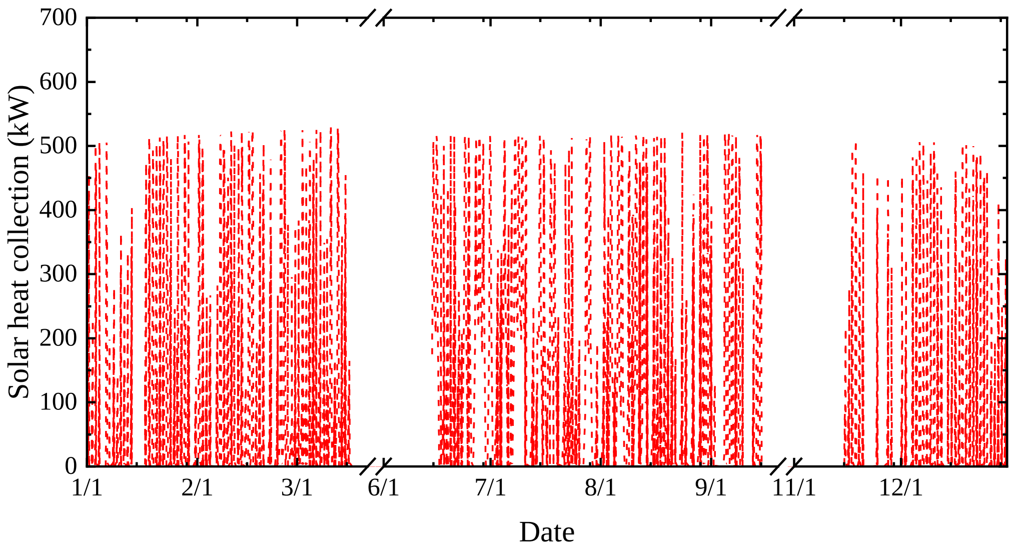

Fig. 11 Hourly solar heat collection of the SHC system

As described in Section 2, the SHC system can be powered by solar thermal and gas fired independently or simultaneously, depending on the intensity of the solar radiation. The solar heat collection accounts for 30.7% of the total heat requirement of the system during cooling period and 23.2% during heating period. The proportions will be more impressive in the areas with rich solar energy. By contrast, the conventional gas-driven absorption heating and cooling system (GHC) is completely dependent on natural gas. Therefore, benefited from the solar heat collection, certain advantages in natural gas saving is found in the SHC system. The total annual natural gas consumption of the SHC system and the GHC system is presented in Fig. 12.

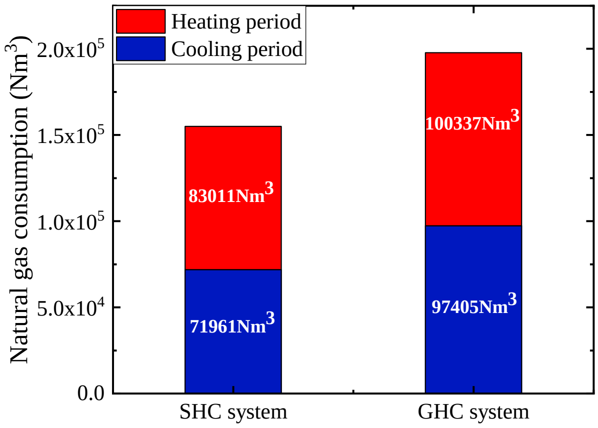

Fig. 12 Total annual natural gas consumption

The natural gas consumption of the SHC system is 71961Nm^3 during cooling period and 83011Nm^3 during heating period, with the total annual natural gas consumption of 154972Nm^3. For the GHC system, the natural gas consumption during cooling period and heating period are 97405Nm^3 and 100337Nm^3 respectively, with the total of 197742Nm^3. Compared with the GHC system, the natural gas saving of the SHC system is 25444Nm^3 in cooling condition and 17326Nm^3 in heating condition, accounting for 35.4% and 20.9% of the gas consumption of the system in the correspondingly period. Fig. 13 presents the hourly natural gas saving of the SHC system. As a whole, the total annual natural gas saving of the SHC system is 42770Nm^3, accounting for 27.6% of the gas consumption of the system.

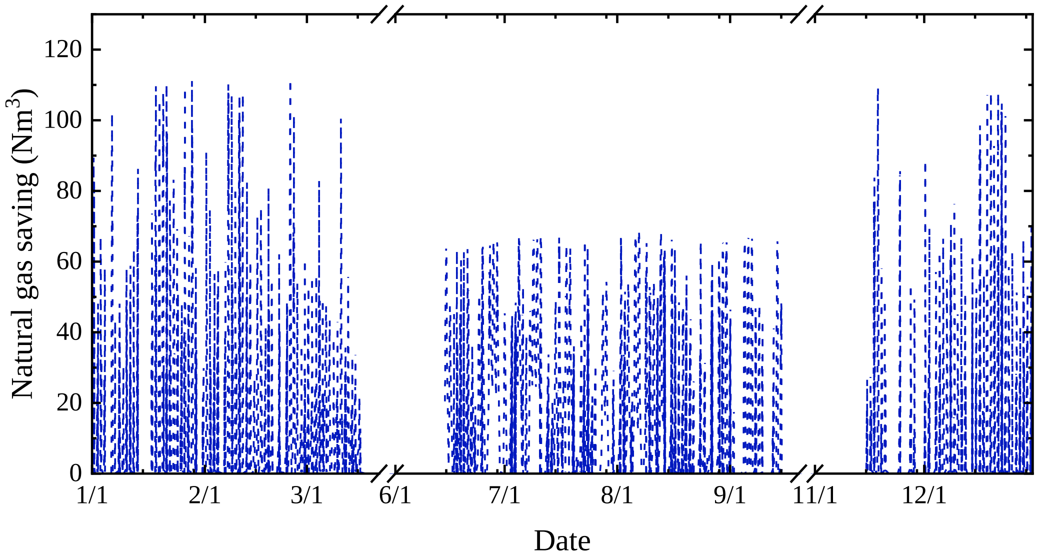

Fig. 13 Hourly natural gas saving of the SHC system

The hourly natural gas consumption of the SHC system and GHC system are presented in Fig. 14 (a) and (b). Since there is a positive relationship between cooling load and solar irradiance intensity, peak-shaving effect on natural gas consumption is achieved under the SHC system in cooling condition, thus fully ensure the operational reliability during the peak load period. More specifically, the peak consumption of natural gas during cooling period of the SHC system is 156Nm^3/h, and the proportion in excess of 100Nm^3/h is 16.1%, which is much lower than the 38.6% of the GHC system. During the heating period, considering the (1) efficiency of plate heat exchanger and gas burner are less than 1 in practical; (2) weak solar irradiance during winter in this area; (3) inverse relationship between thermal load and solar irradiance intensity, the unobvious effect of peak balance can be explained.

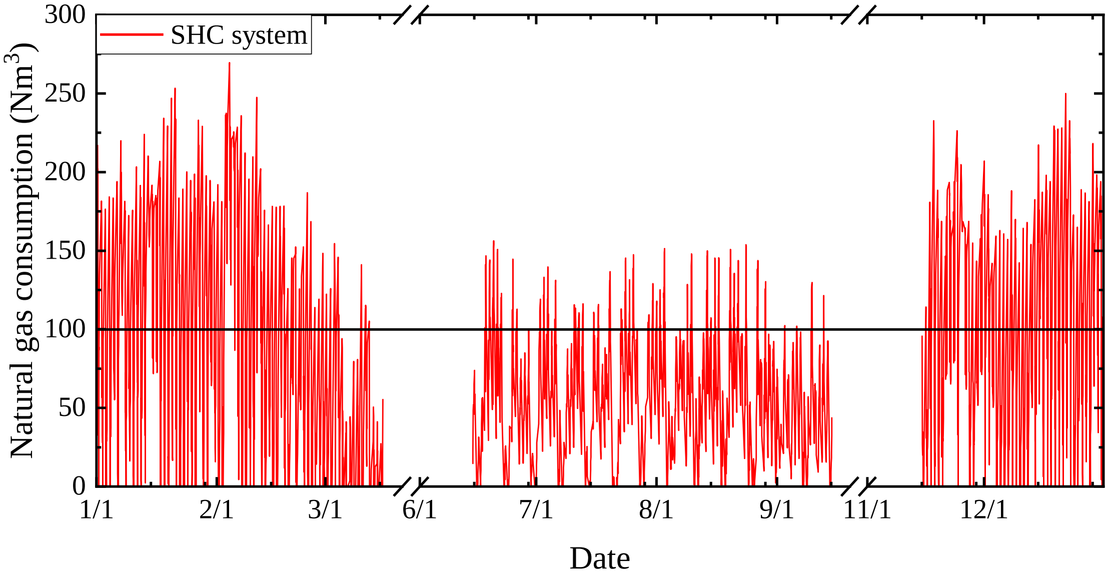

(a) Hourly natural gas consumption of SHC system

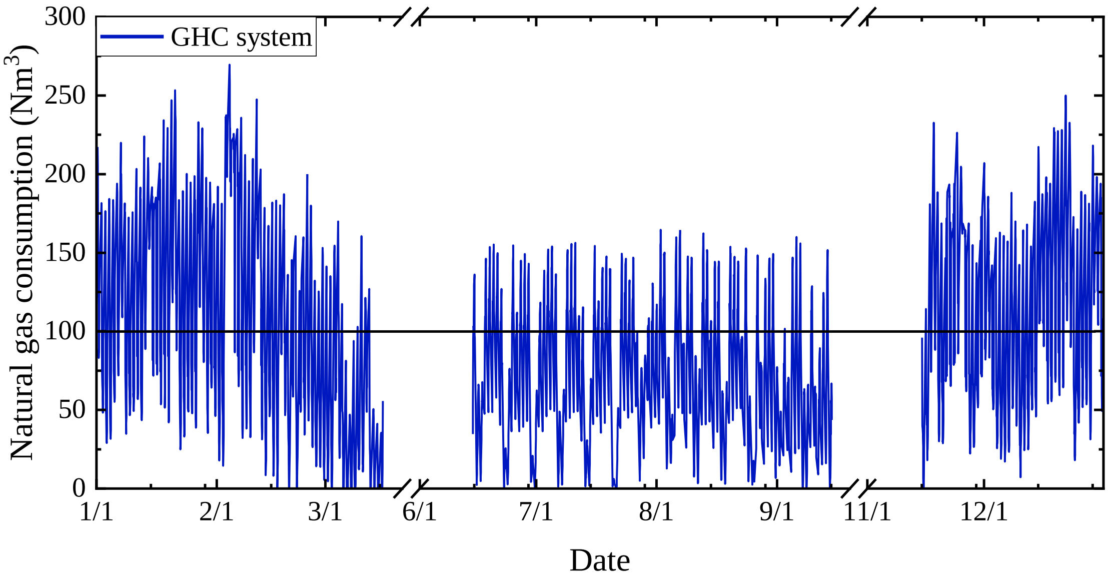

(b) Hourly natural gas consumption of GHC system

Fig. 14 Hourly natural gas consumption of SHC system and GHC system

Except for the natural gas consumption, the electricity consumption is also calculated, which mainly dominates by chiller unit (both in the SHC system and the GHC system) and the solar system related equipments (in the SHC system only). And the solar system related equipments include the solar collector loop pump and the tracking system, etc. As shown in Fig. 15 (a), there is not too much difference in unit power consumption between the two systems, with 14150kWh for SHC system and 14670kWh for GHC system. Considering the variety of heating and cooling loads, the intensity of the solar radiation as well as the COP of the absorption chiller, the difference in electricity consumption of the unit during the heating and cooling period is obvious. Fig. 15 (b) presents the extra electricity consumption of the solar system related equipments in the SHC system, of which 12880kWh is during cooling period and 11060kWh is during heating period, with the total of 23940kWh. Since there is little fluctuation of electricity consumption for this part, the basically similar amount of electricity consumption during heating and cooling period is found.

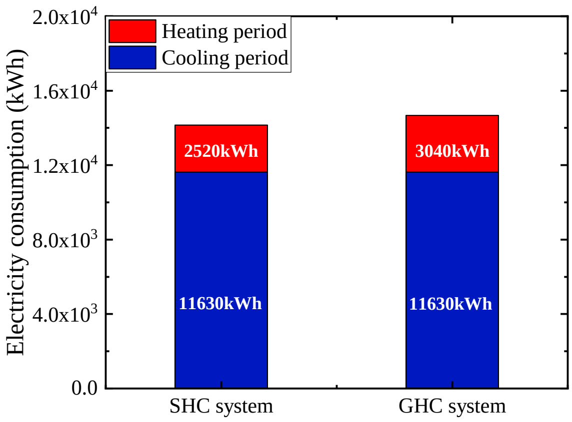

(a) Electricity consumption of the unit

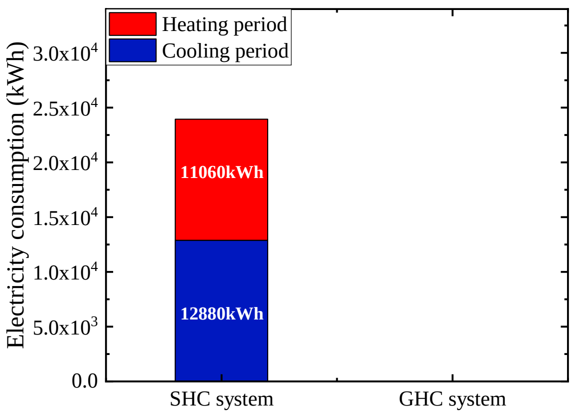

(b) Electricity consumption of solar system related equipments

Fig. 15 Total annual electricity consumption of the SHC system and GHC system

In this paper, the primary energy factors of electricity (PEF_{E}) and natural gas (PEF_{NG}) are 3.58 and 1.64 respectively, and the burner combustion ratio of the absorption chiller adopt 70%, which means 70% of the total natural gas calorific value is consumed and used for the system. According to the calculation by Eqs. (33) to (35), the annual PEC of the SHC system and GHC system are 1915MWh/year and 2323MWh/year, respectively. Thus the PES of the SHC system is 408MWh/year, accounting for 21.3% of the total primary energy consumption, which shows obvious energy saving benefit.

The energy saving potential of the SHC system is also shown by the calculation of PER. The PER of the SHC system is 1.49 during the cooling period and 1.055 during the heating period, while the PER of the GHC are 1.177 and 0.911 respectively.

5.2 Economic performance

To carry out an economic analysis, various financial assumptions are made, as summarized in Table 4.

Table 4

Financial assumptions for economic calculation

Items	Values
PTC	1000RMB/m^2
Intelligent control system	50000RMB/suit
Tracking system	8000RMB/suit
Solar loop pump	4000RMB/suit
Plate heat exchanger	30000RMB/suit
Natural gas	2.66RMB/Nm^3
Electricity	0.68RMB/kWh

The extra initial cost of the SHC system dominates by the solar collecting related configurations. The cost is 1176 thousand RMB according to the calculation. The operating costs mainly include the natural gas cost and the electricity cost. After calculation, A_{ref} and A_{SCH} are 438 thousand RMB and 536 thousand RMB respectively, which demonstrates the advantage of the SHC system in operating cost reduction. The calculated PBP of the SHC system is 12 years. Since the cost of the PTC collectors account for 85% of the total investment, with the unit price of the PTC (per square meter) dropping by 50%, the initial investment will drop by 42.5% to 676 thousand RMB, and the PBP will be reduced to 6.9 years. And according to the analysis in Section 5.1, the additional capital investment cost of the SHC system will be compensated over time due to cumulative savings from energy cost. Therefore, with the decrease of the collector unit price and the increase of energy price, SHC system would be more economically attractive.

5.3 Environmental performance

According to the calculation, the annual CDE of the SHC system and GHC system are 223ton/year and 264ton/year, respectively. Thus the CO_2 emission reduction of the SCH system is 42ton/year, accounting for 18.8% of the total CO_2 emission, which shows considerable emission reduction effect.

6. Conclusions

In this paper, a comprehensive study on an integrated solar heating and cooling (SHC) system driven by double-effect H_2O/LiBr absorption chiller and parabolic trough collectors (PTC) was carried out. The operational modes during the cooling period and heating period were proposed. The heat transfer models of the whole system including the PTC, the double-effect absorption chiller and the plate heat exchanger (PHE) were developed and validated, according to the analysis of seven main heat exchangers of the absorption chiller and heat transfer mechanism of the PTC and PHE. To assess the performances of the system, simulations based on a building model were carried out. Annual performances as well as energetic, economic and environmental (3E) assessments of the SHC system were investigated compared with conventional gas-driven absorption heating and cooling (GHC) system. The following results have been conducted.

- The proposed mathematical models are validated against the field test results with good agreement. The maximum deviation of heat-transfer oil outlet temperature is

0.55℃ at cooling condition and 0.87℃ at heating condition. The simulated efficiency is slightly higher than the measured ones with a difference lower than 5.4%. The maximum deviation of COP between simulated results and test measurements is 0.04, accounted for 3.7% error. The comparison results indicate that the proposed mathematical models are acceptable for the performance analysis of the SHC system.

- A basically 500kW of peak solar heat collection during cooling and heating period is illustrated. And the more stable heat collection ability during cooling period than that during heating period could provide an ideal heat source for the double-effect absorption chiller to cover building loads.
- The SHC system is potential in peak-shaving on natural gas consumption. The peak consumption of natural gas during cooling period is 156Nm^3/h, and the proportion in excess of 100Nm^3/h is 16.1%, which is much lower than the 38.6% of the GHC system.
- The SHC system has certain advantages in energy saving. The solar heat collection accounts for 30.7% of the total heat requirement of the system during cooling period and 23.2% during heating period. Compared with the GHC system, the annual natural gas saving is 42770Nm^3, accounting for 27.6% of the gas consumption of the system. The primary energy saving (PES) of the SHC system is 408MWh/year, accounting for 21.3% of the total primary energy consumption. The primary energy ratio (PER) of the SHC system is 1.49 during the cooling

period and 1.055 during the heating period, while the PER of the GHC are 1.177 and 0.911 respectively.

- The SHC system has potential optimistic economic viability. The payback period (PBP) of the SHC system is 12 years and the cost of the PTC collector is found to be the key parameter impacting the PBP which accounts for 85% of the total investment. With the unit price of PTC (per square meter) dropping by 50%, the initial investment will drop by 42.5%, and the PBP will be reduced to 6.9 years. Therefore, with the unit price of collector decreasing and the energy price increasing, SHC system would be more economically attractive.
- The SHC system shows considerable emission reduction effect. Obvious CO_2 emission reduction with 42ton/year is shown in SCH system, which accounts for 18.8% of the total CO_2 emission.

Reference

[1] R. Hitchin, C. Pout, D. Butler, Realisable 10-year reductions in European energy consumption for air conditioning, Energy Build. 86 (2015) 478–491. doi:10.1016/j.enbuild.2014.10.047.

[2] F.A. Boyaghchi, P. Heidarnejad, Thermoeconomic assessment and multi objective optimization of a solar micro CCHP based on Organic Rankine Cycle for domestic application, Energy Convers. Manag. 97 (2015) 224–234. doi:10.1016/j.enconman.2015.03.036.

[3] Z. Sayadi, N. Ben Thameur, M. Bourouis, A. Bellagi, Performance optimization of solar driven small-cooled absorption-diffusion chiller working with light hydrocarbons, Energy Convers. Manag. 74 (2013) 299–307. doi:10.1016/j.enconman.2013.05.029.

[4] A. Buonomano, F. Calise, A. Palombo, Solar heating and cooling systems by absorption and adsorption chillers driven by stationary and concentrating photovoltaic/thermal solar collectors: Modelling and simulation, Renew. Sustain. Energy Rev. 82 (2018) 1874–1908. doi:10.1016/j.rser.2017.07.056.

[5] A. Aliane, S. Abboudi, C. Seladji, B. Guendouz, An illustrated review on solar absorption cooling experimental studies, Renew. Sustain. Energy Rev. 65 (2016) 443–458. doi:10.1016/j.rser.2016.07.012.

[6] D.N. Nkwetta, J. Sandercock, A state-of-the-art review of solar air-conditioning systems, Renew. Sustain. Energy Rev. 60 (2016) 1351–1366. doi:10.1016/j.rser.2016.03.010.

[7] I. Sarbu, C. Sebarchievici, Review of solar refrigeration and cooling systems, Energy Build. 67 (2013) 286–297. doi:10.1016/j.enbuild.2013.08.022.

[8] T.S. Ge, R.Z. Wang, Z.Y. Xu, Q.W. Pan, S. Du, X.M. Chen, T. Ma, X.N. Wu, X.L. Sun, J.F.

Chen, Solar heating and cooling: Present and future development, Renew. Energy. 126 (2018) 1126–1140. doi:10.1016/j.renene.2017.06.081.

[9] M. Raisul Islam, K. Sumathy, S. Ullah Khan, Solar water heating systems and their market trends, Renew. Sustain. Energy Rev. 17 (2013) 1–25. doi:10.1016/j.rser.2012.09.011.

[10] W. Wu, B. Wang, W. Shi, X. Li, An overview of ammonia-based absorption chillers and heat pumps, Renew. Sustain. Energy Rev. 31 (2014) 681–707. doi:10.1016/j.rser.2013.12.021.

[11] H.Z. Hassan, A.A. Mohamad, A review on solar cold production through absorption technology, Renew. Sustain. Energy Rev. 16 (2012) 5331–5348. doi:10.1016/j.rser.2012.04.049.

[12] A. Allouhi, T. Kousksou, A. Jamil, P. Bruel, Y. Mourad, Y. Zeraouli, Solar driven cooling systems: An updated review, Renew. Sustain. Energy Rev. 44 (2015) 159–181. doi:10.1016/j.rser.2014.12.014.

[13] A. Ghafoor, A. Munir, Worldwide overview of solar thermal cooling technologies, Renew. Sustain. Energy Rev. 43 (2015) 763–774. doi:10.1016/j.rser.2014.11.073.

[14] A. Shirazi, R.A. Taylor, S.D. White, G.L. Morrison, Multi-effect Absorption Chillers Powered by the Sun: Reality or Reverie, in: Energy Procedia, The Author(s), 2016: pp. 844–856. doi:10.1016/j.egypro.2016.06.251.

[15] A. Shirazi, R.A. Taylor, S.D. White, G.L. Morrison, A systematic parametric study and feasibility assessment of solar-assisted single-effect, double-effect, and triple-effect absorption chillers for heating and cooling applications, Energy Convers. Manag. 114 (2016) 258–277. doi:10.1016/j.enconman.2016.01.070.

[16] R. Gomri, Investigation of the potential of application of single effect and multiple effect absorption cooling systems, Energy Convers. Manag. 51 (2010) 1629–1636. doi:10.1016/j.enconman.2009.12.039.

[17] S. Suman, M. Kaleem, M. Pathak, Performance enhancement of solar collectors — A review, Renew. Sustain. Energy Rev. 49 (2015) 192–210. doi:10.1016/j.rser.2015.04.087.

[18] Cabrera F J , FernándezGarcía, A, Silva R M P, Use of parabolic trough solar collectors for solar refrigeration and air-conditioning applications, Renew. Sustain. Energy Rev. 20 (2013) 103–118. doi:10.1016/j.rser.2012.11.081.

[19] M.U. Siddiqui, S.A.M. Said, A review of solar powered absorption systems, Renew. Sustain. Energy Rev. 42 (2015) 93–115. doi:10.1016/j.rser.2014.10.014.

[20] I. Sarbu, C. Sebarchievici, General review of solar-powered closed sorption refrigeration systems, Energy Convers. Manag. 105 (2015) 403–422. doi:10.1016/j.enconman.2015.07.084.

[21] S. Bahria, M. Amirat, A. Hamidat, M. El Ganaoui, M. Slimani, Parametric study of solar heating and cooling systems in different climates of Algeria – A comparison between conventional and high-energy-performance buildings, Energy. 113 (2016) 521–535. doi:10.1016/j.energy.2016.07.022.

[22] S.A.M. Said, M.A.I. El-Shaarawi, M.U. Siddiqui, Analysis of a solar powered absorption system, Energy Convers. Manag. 97 (2015) 243–252. doi:10.1016/j.enconman.2015.03.046.

[23] G. Leonzio, Solar systems integrated with absorption heat pumps and thermal energy storages: state of art, Renew. Sustain. Energy Rev. 70 (2017) 492–505. doi:10.1016/j.rser.2016.11.117.

[24] A. Shirazi, R.A. Taylor, G.L. Morrison, S.D. White, Solar-powered absorption chillers: A

comprehensive and critical review, Energy Convers. Manag. 171 (2018) 59–81. doi:10.1016/j.enconman.2018.05.091.

[25] E. Bellos, C. Tzivanidis, Energetic and financial analysis of solar cooling systems with single effect absorption chiller in various climates, Appl. Therm. Eng. 126 (2017) 809–821. doi:10.1016/j.applthermaleng.2017.08.005.

[26] U. Eicker, D. Pietruschka, M. Haag, A. Schmitt, Systematic design and analysis of solar thermal cooling systems in different climates, Renew. Energy. 80 (2015) 827–836. doi:10.1016/j.renene.2015.02.019.

[27] E. Bellos, C. Tzivanidis, Alternative designs of parabolic trough solar collectors, Prog. Energy Combust. Sci. 71 (2019) 81–117. doi:10.1016/j.pecs.2018.11.001.

[28] E. Bellos, C. Tzivanidis, Assessment of the thermal enhancement methods in parabolic trough collectors, Int. J. Energy Environ. Eng. 9 (2018) 59–70. doi:10.1007/s40095-017-0255-3.

[29] E. Bellos, C. Tzivanidis, V. Belessiotis, Daily performance of parabolic trough solar collectors, Sol. Energy. 158 (2017) 663–678. doi:10.1016/j.solener.2017.10.038.

[30] E. Bellos, C. Tzivanidis, K.A. Antonopoulos, A detailed working fluid investigation for solar parabolic trough collectors, Appl. Therm. Eng. 114 (2017) 374–386. doi:10.1016/j.applthermaleng.2016.11.201.

[31] A. Shirazi, R.A. Taylor, G.L. Morrison, S.D. White, A comprehensive, multi-objective optimization of solar-powered absorption chiller systems for air-conditioning applications, Energy Convers. Manag. 132 (2017) 281–306. doi:10.1016/j.enconman.2016.11.039.

[32] Z.Y. Xu, R.Z. Wang, H.B. Wang, Experimental evaluation of a variable effect LiBr-water

absorption chiller designed for high-efficient solar cooling system, Int. J. Refrig. 59 (2015) 135–143. doi:10.1016/j.ijrefrig.2015.07.019.

[33] S.C. Kaushik, A. Arora, Energy and exergy analysis of single effect and series flow double effect water-lithium bromide absorption refrigeration systems, Int. J. Refrig. 32 (2009) 1247–1258. doi:10.1016/j.ijrefrig.2009.01.017.

[34] E. Bellos, C. Tzivanidis, K.A. Antonopoulos, Exergetic, energetic and financial evaluation of a solar driven absorption cooling system with various collector types, Appl. Therm. Eng. 102 (2016) 749–759. doi:10.1016/j.applthermaleng.2016.04.032.

[35] M.J. Tierney, Options for solar-assisted refrigeration-Trough collectors and double-effect chillers, Renew. Energy. 32 (2007) 183–199. doi:10.1016/j.renene.2006.01.018.

[36] M. Qu, H. Yin, D.H. Archer, A solar thermal cooling and heating system for a building: Experimental and model based performance analysis and design, Sol. Energy. 84 (2010) 166–182. doi:10.1016/j.solener.2009.10.010.

[37] V. Drosou, P. Kosmopoulos, A. Papadopoulos, Solar cooling system using concentrating collectors for office buildings: A case study for Greece, Renew. Energy. 97 (2016) 697–708. doi:10.1016/j.renene.2016.06.027.

[38] J. Wang, R. Yan, Z. Wang, X. Zhang, G. Shi, Thermal Performance Analysis of an Absorption Cooling System Based on Parabolic Trough Solar Collectors, Energies. 11 (2018) 2679. doi:10.3390/en11102679.

[39] F.A. Ghaith, H. ul H. Razzaq, Performance of solar powered cooling system using Parabolic Trough Collector in UAE, Sustain. Energy Technol. Assessments. 23 (2017) 21–32.

doi:10.1016/j.seta.2017.08.005.

[40] M. Balghouthi, M.H. Chahbani, A. Guizani, Investigation of a solar cooling installation in Tunisia, Appl. Energy. 98 (2012) 138–148. doi:10.1016/j.apenergy.2012.03.017.

[41] E. Bellos, C. Tzivanidis, S. Pavlovic, V. Stefanovic, Thermodynamic investigation of LiCl-H2O working pair in a double effect absorption chiller driven by parabolic trough collectors, Therm. Sci. Eng. Prog. 3 (2017) 75–87. doi:10.1016/j.tsep.2017.06.005.

[42] A. Shirazi, R.A. Taylor, S.D. White, G.L. Morrison, Transient simulation and parametric study of solar-assisted heating and cooling absorption systems: An energetic, economic and environmental (3E) assessment, Renew. Energy. 86 (2016) 955–971. doi:10.1016/j.renene.2015.09.014.

[43] M.S.A. Khan, A.W. Badar, T. Talha, M.W. Khan, F.S. Butt, Configuration based modeling and performance analysis of single effect solar absorption cooling system in TRNSYS, Energy Convers. Manag. 157 (2018) 351–363. doi:10.1016/j.enconman.2017.12.024.

[44] O. Behar, A. Khellaf, K. Mohammedi, A novel parabolic trough solar collector model - Validation with experimental data and comparison to Engineering Equation Solver (EES), Energy Convers. Manag. 106 (2015) 268–281. doi:10.1016/j.enconman.2015.09.045.

[45] P.D. Tagle-Salazar, K.D.P. Nigam, C.I. Rivera-Solorio, Heat transfer model for thermal performance analysis of parabolic trough solar collectors using nanofluids, Renew. Energy. 125 (2018) 334–343. doi:10.1016/j.renene.2018.02.069.

[46] Alberto D L C , Roca L , Bonilla J, Dynamic modeling and simulation of a double-effect absorption heat pump, Int. J. Refrig. 72 (2016) 171–191. doi:10.1016/j.ijrefrig.2016.07.018.

[47] M. Fan, H. Liang, S. You, H. Zhang, B. Yin, X. Wu, Applicability analysis of the solar heating system with parabolic trough solar collectors in different regions of China, Appl. Energy. 221 (2018) 100–111. doi:10.1016/j.apenergy.2018.03.137.

[48] A.A. Hachicha, I. Rodríguez, R. Capdevila, A. Oliva, Heat transfer analysis and numerical simulation of a parabolic trough solar collector, Appl. Energy. 111 (2013) 581–592. doi:10.1016/j.apenergy.2013.04.067.

[49] Dudley V E, Kolb G J, Mahoney A R, et al. Test results: SEGS LS-2 solar collector. Nasa Sti/recon Technical Report N, 1994, 96(4):2506–2514.

[50] R.V. Padilla, G. Demirkaya, D.Y. Goswami, E. Stefanakos, M.M. Rahman, Heat transfer analysis of parabolic trough solar receiver, Appl. Energy. 88 (2011) 5097–5110. doi:10.1016/j.apenergy.2011.07.012.

[51] Padilla V. Simplified methodology for designing parabolic trough solar power plants [PhD thesis]. University of South Florida; 2011.

[52] L. Xu, Z. Wang, X. Li, G. Yuan, F. Sun, D. Lei, Dynamic test model for the transient thermal performance of parabolic trough solar collectors, Sol. Energy. 95 (2013) 65–78. doi:10.1016/j.solener.2013.05.017.

[53] Duffie A, Beckman A. Solar engineering of thermal processes. 2nd ed. New York: Wiley; 1991.

[54] Churchill S W , Chu H H S . Correlating equations for laminar and turbulent free convection from a vertical plate. Int. J. Heat Mass Transf 1975; 18(11):1323-1329.

[55] A. Žukauskas. Heat Transfer from Tubes in Crossflow[J]. Advances in Heat Transfer 1987;

18:87-159.

[56] Forristall R. Heat transfer analysis and modeling of a parabolic trough solar receiver implemented in engineering equation solver. NREL/TP-550-34169, 2003.

[57] S.A. Kalogirou, A detailed thermal model of a parabolic trough collector receiver, 2012. doi:10.1016/j.energy.2012.06.023.

[58] E. Bellos, C. Tzivanidis, K.A. Antonopoulos, Exergetic and energetic comparison of LiCl-H2O and LiBr-H2O working pairs in a solar absorption cooling system, Energy Convers. Manag. 123 (2016) 453–461. doi:10.1016/j.enconman.2016.06.068.

[59] W. Zheng, J. Yang, H. Zhang, S. You, Simulation and optimization of steam operated double effect water-LiBr absorption heat pump, Appl. Therm. Eng. 109 (2016) 454–465. doi:10.1016/j.applthermaleng.2016.08.113.

[60] Y. Guo, F. Wang, M. Jia, S. Zhang, Modeling of plate heat exchanger based on sensitivity analysis and model updating, Chem. Eng. Res. Des. 138 (2018) 418–432. doi:10.1016/j.cherd.2018.09.004.

[61] Coleman T F , Li Y . On the convergence of interior-reflective Newton methods for nonlinear minimization subject to bounds. Mathematical Programming 1994; 67(1-3):189-224.

[62] R.S. Moghadam, H. Sayyaadi, H. Hosseinzade, Sizing a solar dish Stirling micro-CHP system for residential application in diverse climatic conditions based on 3E analysis, Energy Convers. Manag. 75 (2013) 348–365. doi:10.1016/j.enconman.2013.06.008.

[63] M. Fan, H. Liang, S. You, H. Zhang, B. Yin, X. Wu, Performance analysis of a solar heating system with the absorption heat pump and oil/water heat exchanger, in: Energy Procedia,

Elsevier B.V., 2017: pp. 97–104. doi:10.1016/j.egypro.2017.12.016.

[64] U. Desideri, S. Proietti, P. Sdringola, Solar-powered cooling systems: Technical and economic analysis on industrial refrigeration and air-conditioning applications, Appl. Energy. 86 (2009) 1376–1386. doi:10.1016/j.apenergy.2009.01.011.

[65] A.H. Mosaffa, L.G. Farshi, C.A. Infante Ferreira, M.A. Rosen, Exergoeconomic and environmental analyses of CO2/NH3 cascade refrigeration systems equipped with different types of flash tank intercoolers, Energy Convers. Manag. 117 (2016) 442–453. doi:10.1016/j.enconman.2016.03.053.

[66] L. Yang, J.C. Lam, J. Liu, Analysis of typical meteorological years in different climates of China, Energy Convers. Manag. 48 (2007) 654–668. doi:10.1016/j.enconman.2006.05.016.